Handbook of Chemistry and Physics (1963). p. 2378. Cleveland: Chemical Rubber Publishing Co.
JEFFREY, G. A., PARRY, G. S. & MOZZI, R. L. (1956). *J. Chem. Phys.* **25**, 1024.
KNIPPENBERG, W. F. (1963). *Philips Res. Reports*, **18**, 271.
KNIPPENBERG, W. F. & GOMES DE MESQUITA, A. H. (1965). *Z. Kristallogr.* **121**, 67.
LOMBARDI, E. & JANSEN, L. (1965). *Phys. Rev.* **140**, A 275.
SCHNEER, C. J. (1955). *Acta Cryst.* **8**, 279.
SCHUYFF, A. & HULSCHER, J. B. (1965). *Rev. Sci. Instrum.* **36**, 957.
SPITZER, W. G., KLEINMAN, D. A., FROSCH, C. J. & WALSH, D. J. (1959). *Proc. Conf. Silicon Carbide, Boston*, p. 347. New York: Pergamon Press (1960).
TAYLOR, A. & JONES, R. M. (1959). *Proc. Conf. Silicon Carbide, Boston*, p. 147. New York: Pergamon Press (1960).
VERMA, A. R. & KRISHNA, P. (1966). *Polymorphism and Polytypism in Crystals*, New York: John Wiley.
ZACHARIASEN, W. (1963). *Acta Cryst.* **16**, 1139.

Acta Cryst. (1967). **23**, 617

The Crystal Structure at 220 °C of Orthorhombic High Tridymite from the Steinbach Meteorite

BY W. A. DOLLASE*
Massachusetts Institute of Technology, Cambridge, Massachusetts, U.S.A.

(*Received* 15 *February* 1967)

Tridymite from the Steinbach meteorite has been examined at 220 °C and found to be orthorhombic, space group $C222_1$ with $a=8{\cdot}74$, $b=5{\cdot}04$, $c=8{\cdot}24$ Å. The crystal structure has been determined and refined, using single-crystal counter-diffractometer data, to $R=8{\cdot}6\%$. The resulting structure, though similarly connected, is distorted in comparison with the ideal high-tridymite structure. The tetrahedra remain nearly regular but are rotated from the ideal positions. The oxygen atoms show strong disorder which is interpreted as thermal in origin. The magnitudes of the thermal displacements, especially of the oxygen atoms normal to their bonds with silicon atoms, are unusually large, amounting to 0·4 Å.

Introduction

Tridymite, a polymorph of SiO_2, is known from numerous sources (meteorites, refractory silica brick, natural terrestrial occurrences with widely different temperatures of formation, and from numerous diverse syntheses). The variation in diffraction effects observed with crystals from different sources suggests the existence of several different types of tridymite. The (only) three meteoritic and (only) two silica brick tridymites examined to date using single-crystal methods (Dollase & Buerger, 1966) give identical results and constitute the tridymite type considered here. On the basis of an existing chemical analysis the Steinbach meteoritic tridymite was chosen for further structural studies of this tridymite type.

Tridymite from the Steinbach meteorite was found, from film and single-crystal diffractometer observations, to exist in three well defined structural states between room temperature and 250 °C. Each of the phases is characterized by a different cell and symmetry (Dollase & Buerger, 1966; Hoffman, 1967). The room-temperature phase is monoclinic, *Cc* or *C*2/*c*, with $a=18{\cdot}54$, $b=5{\cdot}00$, $c=23{\cdot}83$ Å, $\beta=105{\cdot}7°$. Above about 107 °C this phase transforms reversibly to a phase which shows a cell dimensionally similar to that reported for high tridymite (see below). Photographs taken above this temperature, however, reveal that the reciprocal-lattice points corresponding to this small cell are accompanied by satellites in the pseudohexagonal **a*** direction which are faint, though sharp, and whose spacing indicates a true periodicity that apparently varies continuously from about 105 Å at 107 °C to about 65 Å at 180 °C; at this temperature the satellites fade into the background. The origin of the satellites is tentatively assigned to strongly correlated thermal motion of the type postulated to account for similar observations in $NaNO_2$ (Tanisaki, 1963).

The polymorph existing from about 180 °C to beyond the 250° limit of the investigated temperature range, is here termed orthorhombic high tridymite since it shows the same small cell (though different symmetry) that has been reported for high tridymite (Gibbs, 1927). This paper reports the results of a study of its crystal structure at 220 °C.

Previous structural studies of high tridymite

The first structural study of tridymite was that of high tridymite made by R. E. Gibbs in 1927. The source of the tridymite was not given. The unit-cell parameters were measured from Laue and oscillation photographs taken at an undetermined temperature 'well above the transition point'. Gibbs concluded that at this temperature the Laue symmetry was *6mmm*, and that the reflections of the type *hh.l*, $l=2n+1$ were absent. By requiring the structure to be composed of regular SiO_4

* Present address: Department of Geology, University of California, Los Angeles, California.

tetrahedra, the space group could be limited to $P6_3/mmc$. As noted by Gibbs, this fixed the structure as essentially identical with that of hexagonal ice.

The only other structural investigation made of tridymite above room temperature was a powder-diffraction study of a natural volcanic tridymite by Sato (1964). He reported that he observed 'good agreement' of the values calculated from the model proposed by Gibbs and 23 intensities measured on a powder diffractometer at 500°C.

Symmetry of orthorhombic high tridymite

A specimen of tridymite from the Steinbach meteorite was kindly provided by Professor Clifford Frondel from the Harvard Museum collection. A spectrographic analysis showing the unusually high purity of this tridymite is given in Table 1. This material was found to be invariably twinned with the sixfold axis of the pseudohexagonal cell as twin axis. Assuming that the relative volumes of the twin individuals of a given grain do not change while heated to the temperatures under consideration, the proportion of the grain in each of the possible twin orientations is measurable from the relative intensities of the reflections of the low-temperature form which are not superposed by the twinning. By examining several dozen grains it was possible to select one with only 3% of its volume in a twinned position relative to the main part of the grain. The twinning of this grain would thus contribute a maximum error of 1·5% to the observed structure factors, which was considered negligible. Precession and oscillation photographs were taken of this grain and of other less favorably twinned grains at temperatures in the range of 180 to 250°C, using a heating device similar to that described by Wuensch (1965).

Table 1. *Spectrographic analysis of impurities in tridymite from Steinbach meteorite*
(Analyst: Wm. H. Dennen.)

Al	400 ± 50 ppm
Na	270 ± 50
Mg	tr
Fe	tr
K	50
Li	10

The photographs revealed strong hexagonal pseudosymmetry and a cell which is dimensionally hexagonal within the error of measurement. The true symmetry in this temperature range was seen to be orthorhombic, as was later verified from comparison of diffractometer measurements of equivalent reflections, described below. The parameters of the *C*-centered orthorhombic unit cell are $a=8{\cdot}74$, $b=5{\cdot}05$, $c=8{\cdot}24$ Å. With careful attention paid to possible effects of twinning, the diffraction symbol was determined to be $mmmC\ -/-,\ -/-,\ 2_1/-$. The space group is therefore uniquely determined as $C222_1$.

Data collection

Intensity measurements were made on a single-crystal counter-diffractometer employing equi-inclination geometry. The furnace used in heating the crystal was especially designed to hold the temperature constant over the data-collection period and to allow the maximum possible volume of reciprocal space to be explored. In this design the primary and diffracted beams each pass through a sheet of nickel foil 0·0005 inch thick which serves as a heat-radiation barrier and also as a β filter for the copper X-radiation employed. A xenon-filled proportional counter was used with pulse-height analysis to eliminate the electrical noise and also the $\lambda/2$ and shorter-wavelength harmonics.

Integrated intensities were collected by the fixed-counter, rotating-crystal method. The background, which was noted to be unusually high near the peaks, was estimated by fixed-time counts at each end of the scan. Approximately 300 reflections were measured in all. This included all independent reflections within the range of the instrument, as well as about 125 additional reflections used to verify the proposed symmetry and to determine the precision of the measurements. As all reflections were observable, they were uniformly assigned their measured values and treated equally in all subsequent calculations, although later refinement did suggest that the measurement of the weaker reflections was relatively less precise.

The data were corrected for Lorenz and polarization factors, for absorption by the crystal and for absorption by the nickel-foil shield of the furnace. After correcting for these effects, the symmetry-related reflections were compared and found to show an average deviation of 3·3% in intensity from *mmm* symmetry. This corresponds to an average error of less than 2% in the structure factors, and so provides a confirmation of the orthorhombic symmetry at this level of intensity measurement.

Determination and refinement of the structure

It was considered likely that the actual structure of the high form would be similar to the ideal high-tridymite structure proposed by Gibbs. In order to verify this, a Patterson function was first calculated. The positions of the maxima in the resulting maps confirmed the similarity of the general linkage of the ideal high-tridymite structure but showed that the atoms must be shifted from their ideal locations. In particular, the Si–Si vectors could be seen to lie clearly off the Patterson line 00*z* thus proving the absence of a mirror plane normal to the pseudohexagonal *c* axis. Strong smearing of the silicon–oxygen and oxygen–oxygen maxima, relative to the Si–Si maxima also showed that the oxygen atoms were strongly affected by thermal motion or by some other form of disorder.

The locations of the atoms in ideal hexagonal high tridymite expressed in orthorhombic space group

$C222_1$, are given in Table 2. (The origin is taken at the position having symmetry 122_1 which is shifted by $c/4$ from the 212_1 origin adopted for this space group in *International Tables*.) It can be seen that there is one SiO_2 formula unit to be specified. The silicon atom and one of the oxygen atoms are in the general position while two oxygen atoms occur in the special positions 4(*a*) and 4(*b*), which are located on twofold axes.

A structure-factor calculation was made using the values given in Table 2. Scattering curves for un-ionized atoms given in *International Tables for X-ray Crystallography* (1962) were employed throughout. The agreement between the observed and calculated structure amplitudes, in terms of the usual R value, was 42%, which is a measure of the deviation of the intensities from hexagonal symmetry. A full-matrix, least-squares refinement was then carried out for the positional and isotropic thermal parameters, in that order. All reflections were included and weighted equally. The refinement converged in five cycles to $R=13{\cdot}4\%$. The ratio of observations to total variables was more than 13:1. As was expected from the Patterson map, the apparent isotropic temperature factors of all the oxygen atoms were found to be very high, averaging about 7 Å^2.

Table 2. *Atoms in ideal hexagonal high tridymite described in orthorhombic space group* $C222_1$

	Equipoint	x	y	z
Si	8 (*c*)	1/6	1/2	7/16
O(1)	4 (*a*)	1/3	0	*3/4*
O(2)	4 (*b*)	*0*	1/2	*1/2*
O(3)	8 (*c*)	1/4	1/4	1/2

The symmetry-fixed parameters are italicized.

At this point an electron-density function and difference map were computed. The electron-density map, Fig. 1(*a*), clearly indicated that the oxygen atoms were highly elongated. Similarly, the difference map, made with this isotropic thermal motion approximation,

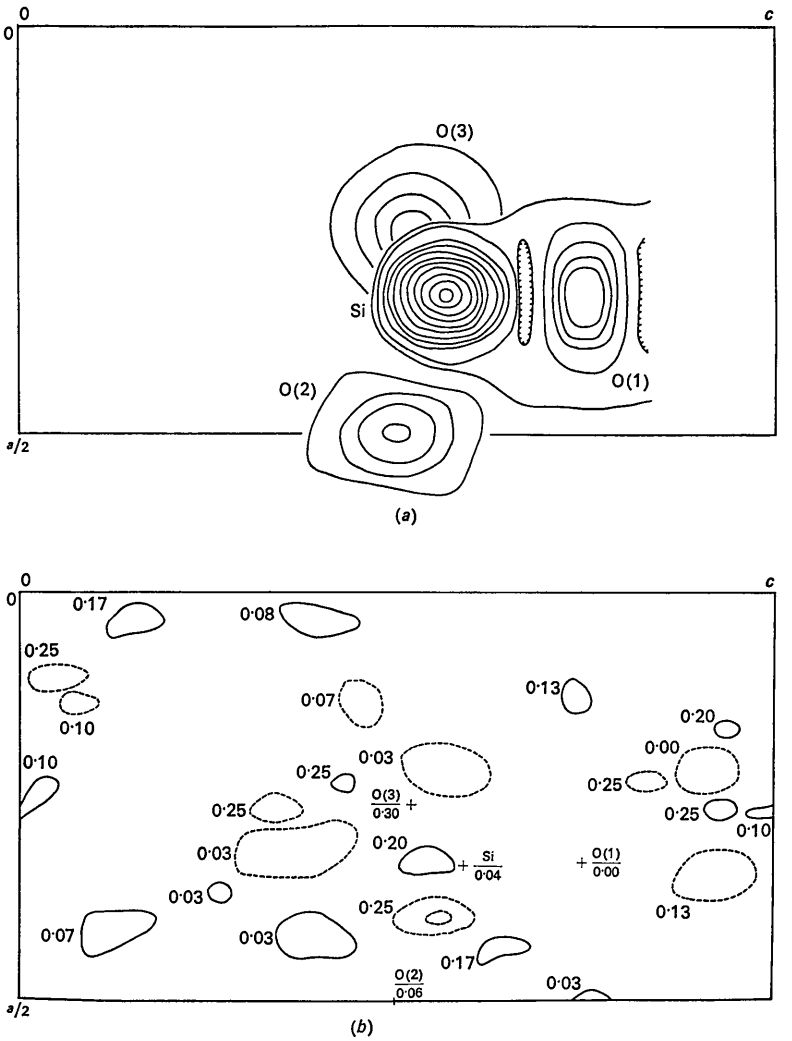

Fig. 1. (*a*) Composite electron density projected along the *b* axis. (*b*) Composite difference map. Contour interval is 0·2 e; negative density is indicated by dashed contours. Numbers refer to *y* coordinates.

showed anomalies corresponding to as much as 0·7 electrons around some of the oxygen-atom locations.

The appearance of the oxygen atoms in these maps, as well as the magnitude of the temperature factors, confirms that the oxygen atoms are disordered, as had been suggested by the Patterson map. The elongated oxygen positions are thus the average positions of these atoms, the averaging being either over time (thermal motion interpretation) or space (static disorder interpretation) or both. No definite decision between these can be made with the evidence at hand. However, since there is no diffraction evidence against a thermal-motion interpretation, and since, as will be shown, a not unreasonable model can be found which adequately accounts for the observed X-ray intensities, this interpretation is adopted here. A static disorder interpretation on the other hand, would require a split-atom model which, because of the apparent 'shape' of the oxygen atoms (described in detail below), would require more than two split atoms to approximate each of the three different oxygen atoms. Such a model would have more variable parameters than a simple thermal motion model and thus was considered less justified.

If the disorder is then considered as thermal in origin, Fig. 1(*a*) shows it to be strongly anisotropic. (O(3) appears isotropic in Fig. 1(*a*) because the Si–O–Si bond is nearly parallel to this projection axis.) Refinement was therefore continued with anisotropic temperature factors. The restrictions to the thermal ellipsoids of the atoms lying on the twofold axes is that, for O(1), $B_{12}=B_{13}=0$, and for O(2), $B_{12}=B_{23}=0$. The refinement converged in three cycles at $R=8{\cdot}6\%$. Employing anisotropic temperature factors, the ratio of observations to total variables is 6:1. The parameter shifts in the last cycle were all less than one-tenth their individual estimated standard deviations. The e.s.d.'s were calculated from the full inverse least-square matrix.

Another electron-density map and difference map were then calculated. The electron-density map was essentially identical with the previous one, showing that few, if any, signs had changed in the anisotropic refinement. The difference map, shown in Fig. 1(*b*), was, however, quite changed from the previous map, and showed no anomalies near any of the atom locations, indicating that the positional disorder was well accounted for by the assumption of large-magnitude, anisotropic thermal motion.

Table 3 lists the final refined positional parameters and their estimated standard deviations. Table 4 lists the final refined thermal parameters in terms of the anisotropic temperature factors, β_{ij}, and their estimated standard deviations. A comparison of the observed structure amplitudes and those calculated from the final model is given in Table 5. Inspection of the individual weaker reflections (especially the 60*u* reflections) shows the agreement in a few cases to be poor. The featureless final difference map, however, suggests these errors are random rather than the effect of any systematic error in the measurements or in the model.

A measure of the statistical significance of the differences between the starting parameters of Table 2 and the final parameters of Table 3 (that is, of the de-

Table 5. *Comparison of observed and calculated structure amplitudes* ($\times 3{\cdot}67$)

hkl	F_o	F_c	hkl	F_o	F_c	hkl	F_o	F_c	hkl	F_o	F_c
020	222	222	531	64	67	203	124	130	025	37	38
040	110	109	551	18	25	223	120	116	045	25	16
060	21	18	601	49	2	243	61	56	115	150	146
110	278	277	621	84	70	313	16	11	135	103	105
130	108	101	641	47	46	333	41	38	155	24	23
150	19	23	711	54	44	353	20	19	205	138	156
200	263	292	731	28	27	403	124	121	225	125	128
220	9	17	801	32	30	423	113	104	245	46	44
240	54	54	821	25	27	443	44	35	315	23	17
310	221	218	911	29	9	513	121	105	335	32	32
330	156	153	931	23	22	533	60	56	355	20	24
350	37	39	1001	14	18	553	20	22	405	127	123
400	17	18				603	25	5	425	102	100
420	116	110	022	39	43	623	34	33	445	37	37
440	35	29	042	62	57	643	17	15	515	106	98
510	121	127	112	143	136	713	72	75	535	46	46
530	61	69	132	82	79	733	36	39	605	19	3
550	9	12	152	45	47	803	60	56	625	15	11
600	168	171	202	130	125	823	39	42	645	17	19
620	137	149	222	77	66	913	10	6	715	60	63
640	43	46	242	66	63	1003	27	36	735	29	32
710	71	75	312	53	54				805	48	46
730	24	28	332	83	76	024	20	8	825	30	35
800	33	30	352	25	22	044	15	21	915	10	8
820	25	38	402	69	63	114	94	96			
910	49	56	422	80	74	134	74	77	026	102	102
930	30	34	442	49	49	154	49	54	046	34	29
1000	11	12	512	73	74	204	65	50	116	62	59
			532	62	61	224	73	70	136	42	39
021	52	52	552	34	34	244	65	67	206	51	51
041	132	139	602	94	97	314	31	27	226	57	68
061	41	48	622	87	93	334	22	23	246	30	32
111	181	178	642	29	27	354	5	4	316	106	109
131	109	108	712	56	52	404	53	47	336	45	45
151	33	37	732	32	35	424	60	56	406	57	63
201	166	170	802	30	14	444	53	56	426	39	33
221	123	114	822	29	29	514	43	23	446	25	32
241	80	82	912	31	34	534	53	52	516	34	32
311	36	31	1002	19	6	604	20	17	536	25	27
331	96	93				624	20	24	606	52	54
351	60	58	023	15	11	644	7	4	626	41	35
401	115	104	043	57	65	714	35	21	716	20	13
421	97	85	113	115	118	734	34	37	806	18	26
441	31	24	133	110	105	804	27	11			
511	92	82	153	26	22	824	28	20			
						914	5	3			

Table 3. *Final positional parameters of orthorhombic high tridymite*

	x	$\sigma(x)$	y	$\sigma(y)$	z	$\sigma(z)$
Si	0·16846	0·00051	0·53589	0·00084	0·43857	0·00070
O(1)	0·3336	0·0031	0	—	0·75	—
O(2)	0	—	0·5597	0·0076	0·5	—
O(3)	0·2547	0·0028	0·3029	0·0031	0·5213	0·0027

Table 4. *Final thermal parameters*

The form of the temperature factor employed is $\exp[-(\beta_{11}h^2+\beta_{22}k^2+\beta_{33}l^2+2\beta_{12}hk+2\beta_{13}hl+2\beta_{23}kl)]$.

	β_{11}	σ	β_{22}	σ	β_{33}	σ	β_{12}	σ	β_{13}	σ	β_{23}	σ
Si	0·0119	0·0006	0·0260	0·0016	0·0119	0·0013	0·0012	0·0010	−0·0001	0·0007	−0·0013	0·0009
O(1)	0·040	0·006	0·080	0·014	0·017	0·007	0	—	0	—	0·009	0·007
O(2)	0·012	0·002	0·136	0·023	0·030	0·007	0	—	0·002	0·003	0	—
O(3)	0·041	0·004	0·054	0·007	0·025	0·004	0·024	0·005	−0·006	0·003	0·008	0·005

viation from the ideal tridymite structure) can be made by comparing these differences with the final standard deviations. It can be seen that the shifts amount to as much as forty standard deviations.

Description of the structure

The final refined structure is illustrated in Fig. 2. In this view the tetrahedra joined in the direction of the *c* axis are seen to be slightly offset from each other in the direction of the *b* axis. This should be compared with the ideal structure where, in this view, these same tetrahedra would project directly on top of one another. Fig. 3 focuses attention on a smaller fragment of the structure as seen looking along the *a* axis. In the ideal structure these tilted pairs of tetrahedra would stand vertically along the *c* axis. The observed tilt, relative to the *c* axis, amounts to about 8°. From the two figures it can be seen that the distortion results in a slight flexure of joined tetrahedra at O(2) and O(3), but that the tetrahedra joined at O(1) are essentially as in ideal high tridymite.

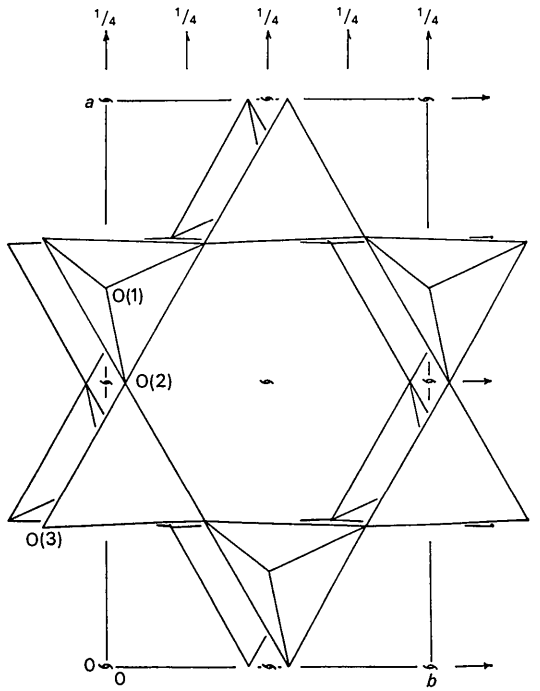

Fig. 2. Projection of the structure of orthorhombic high tridymite along **c**.

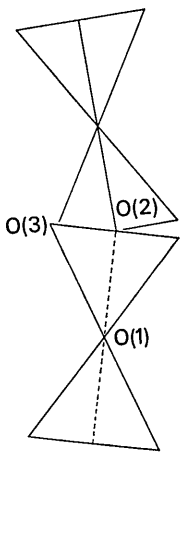

Fig. 3. Tilt of SiO_4 tetrahedra in orthorhombic high tridymite as viewed along **a**.

Bond distances, bond angles, and their standard deviations are listed in Table 6. The values given have not been corrected for the effects of disorder, and thus refer to the average structure as determined by the refinement. In view of the disorder the standard deviations are surprisingly low. The weighted average Si–O distance in the tetrahedron, $\bar{d}_w=(\Sigma\, d_i/\sigma_i/\Sigma\, 1/\sigma_i)$, is 1·56 Å. This should be compared with the distances, 1·603 and 1·616 Å, found in quartz by Zachariasen & Plettinger (1965); and 1·601 and 1·608 Å found in low cristobalite by Dollase (1965). The deviations of the individual bonds from this weighted average is, in each case, less than one standard deviation, implying that the tetrahedron is regular in regard to distances at this level of refinement.

Table 6. *Interatomic distances and angles in orthorhombic high tridymite*

	Bond distances	σ
Si–O(1)	1·563 Å	0·006 Å
Si–O(2)	1·561	0·005
Si–O(3)	1·542	0·017
Si–O(3′)	1·554	0·018
	Bond angles	**σ**
O(1)–Si–O(2)	108·7°	1·4°
O(1)–Si–O(3)	108·6	0·8
O(1)–Si–O(3′)	110·7	1·2
O(2)–Si–O(3)	105·9	0·8
O(2)–Si–O(3)	111·9	0·9
O(3)–Si–O(3′)	110·0	1·5
Si–O(1)–Si	178·7	0·9
Si–O(2)–Si	171·2	2·7
Si–O(3)–Si	165·2	1·4

The deviations of the individual tetrahedral angles from the average (109°27′) are as much as four times the standard deviations of the individual bond angles. This suggests that the tetrahedra do depart slightly from perfect regularity. In the ideal high-tridymite structure the Si–O–Si bond angles are constrained by symmetry to be exactly 180°. In the orthorhombic structure described here the bond angle across O(1) does not depart significantly from this value. The bond angles across O(2) and O(3), are significantly different from 180° and from each other, but both are still large compared with the 'normal' values found in quartz, 143·5° (Zachariasen & Plettinger, 1965) and in low cristobalite, 146·8° (Dollase, 1965).

Table 7. *Root-mean-square amplitudes along principal axes of the thermal ellipsoids, and orientations of the ellipsoids with respect to crystallographic axes*

		r.m.s. amplitude	σ	Angles between axes of ellipsoid, r_i, and crystal $r_i \wedge \mathbf{a}$	$r_i \wedge \mathbf{b}$	$r_i \wedge \mathbf{c}$
Si	a'	0·215 Å	0·005	8±10°	14±6°	94±14°
	b'	0·182	0·006	96±5	12±8	80±9
	c'	0·203	0·011	85±14	100±9	11±9
O(1)	a'	0·394	0·028	0 —	90 —	90 —
	b'	0·324	0·027	90 —	11±11	80±11
	c'	0·238	0·047	90 —	101±11	11±11
O(2)	a'	0·214	0·021	3±6	90 —	93±6
	b'	0·419	0·036	90 —	0 —	90 —
	c'	0·323	0·035	87±6	90 —	3±6
O(3)	a'	0·408	0·015	16±4	75±4	96±5
	b'	0·240	0·018	106±4	27±9	111±11
	c'	0·301	0·024	91±5	68±10	22±10

Table 7 gives the root-mean-square amplitudes of thermal vibration in the directions of the principal axes of the thermal ellipsoids. The angles given are those between the respective principal axes and the crystallographic axes. The principal axis of the ellipsoid which most nearly parallels the crystallographic *a* axis is termed *a'*, and so forth. For comparison the r.m.s. amplitudes, found for quartz, at room temperature, are about 0·08 for Si and 0·09 to 0·14 for oxygen (Zachariasen & Plettinger, 1965). The thermal ellipsoids given in Table 7 are shown plotted in Fig. 4. It can be seen that the silicon atom is nearly spherical but that the oxygen atom ellipsoids all have one shorter axis, the other two being one and one-half to twice as long and both about the same length. The oxygen atom ellipsoids are therefore nearly oblate spheroids. The angles between the Si–O bonds and the principal axes of the respective oxygen atom ellipsoids are given in Table 8. The short axes of the ellipsoids are roughly parallel to their respective Si–O bonds and therefore the longer axes are roughly normal to these bonds.

Table 8. *Angles between individual* Si–O *bonds (S) and the principal axes of their respective oxygen atom thermal ellipsoids*

S	$S \wedge a'$	$S \wedge b'$	$S \wedge c'$
Si–O(1)	91°	86°	*−4°*
Si–O(2)	*−17*	86	106
Si–O(3)	77	*−15*	83
Si–O(3')	80	*12*	98°

The angles to the short axes of the ellipsoids are italicized.

The effect of such thermal motion on the bond lengths can be treated quantitatively (Busing & Levy, 1964) provided a correlation model can be assumed. From the known, high strength of the Si–O bond and from the shape and orientation of the ellipsoids it seems reasonable to assume that the entire Si–O tetrahedron is moving, more or less, in-phase and in addition executing a libration about the Si atom center. This type of correlated motion corresponds to Busing & Levy's atom *B* (oxygen) 'riding' on atom *A* (silicon). The Si–O bond lengths, corrected for such an assumed correlation, are given in Table 9. The values are very nearly those found in the room-temperature structures noted above.

Table 9. *Interatomic distances corrected for 'oxygen riding on silicon'*

	Bond distance
Si–O(1)	1·621 Å
Si–O(2)	1·625
Si–O(3)	1·608
Si–O(3')	1·597
Average	1·61

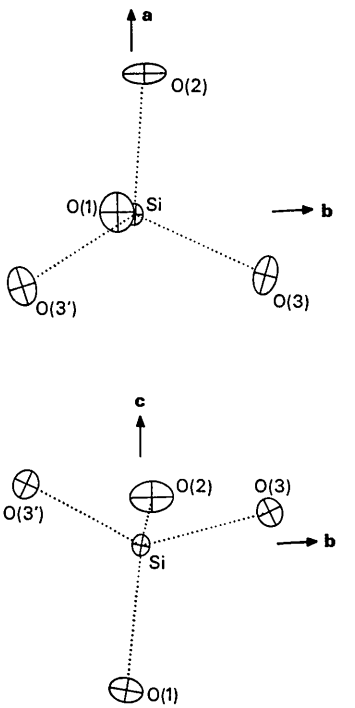

Fig. 4. Projection of the axial components of thermal displacement in orthorhombic high tridymite as viewed along the *c* axis (upper diagram) and along the *a* axis (lower diagram).

The effect of the thermal motion on the tetrahedral bond angles, for the case of this model, would be small. On the other hand the effects on the Si–O–Si angles would require a knowledge of how the tetrahedra are vibrating relative to each other, which is not available. In any event, it can be qualitatively seen that since the time average values of these angles are so large, almost any type of correlated or noncorrelated motion will cause their instantaneous values to be lower and thus more nearly equal to those found in the room temperature structures quoted above.

Summary

The structure of the Steinbach tridymite at 220 °C is distorted relative to the ideal high-tridymite structure. The distortion consists of a twisting of pairs of tetrahedra about the *a* axis such that tetrahedra joined in the *c*-axis direction are alternately displaced in the positive and negative direction of the *b* axis. The amount of the twist, about 8°, causes the centers of the tetrahedra to be displaced by about 0·2 Å. The atoms show strong thermal motion, especially oxygen atoms in the directions roughly normal to the silicon–oxygen bonds. The tetrahedra are very nearly regular and the interatomic distances (and perhaps also the angles) are not too different from those reported for room-temperature structures, provided the thermal motion is taken into account.

The author gratefully acknowledges the interest, advice and support given this study by Professor Martin J. Buerger. The spectrographic analysis was kindly provided by Professor William H. Dennen. This research was supported, in part, by a National Science Foundation grant. The computations were carried out at the Massachusetts Institute of Technology Computation Center.

References

BUSING, W. R. & LEVY, H. A. (1964). *Acta Cryst.* **17**, 142.

DOLLASE, W. A. (1965). *Z. Kristallogr.* **121**, 369.

DOLLASE, W. A. & BUERGER, M. J. (1966). *Program* 1966 *Annual Meeting, Geol. Soc. Amer.*, p. 54.

GIBBS, R. E. (1927). *Proc. Roy. Soc.* A, **113**, 351.

HOFFMAN, W. (1967). *Naturwissenschaften.* In the press.

International Tables for X-ray Crystallography (1962). Vol. III, p. 202. Birmingham: Kynoch Press.

SATO, M. (1964). *Min. J. Japan*, **4**, 115.

TANISAKI, S. (1963). *J. Phys. Soc. Japan*, **18**, 1181.

WUENSCH, B. J. (1964). In BUERGER, M. J. (1964). *The Precession Method*, p. 248. New York: John Wiley.

ZACHARIASEN, W. H. & PLETTINGER, H. A. (1965). *Acta Cryst.* **18**, 710.

Acta Cryst. (1967). **23**, 623

The Crystal and Molecular Structure of 2,5-Dimethyl-2,5-*endo*-thio-1,4-dithiane

BY A. M. O'CONNELL

Crystallography Group, University of Göteborg, Sweden

(*Received* 15 *April* 1967)

The product $C_6H_{10}S_3$, formed when an alcoholic solution of chloroacetone saturated with hydrogen chloride is treated with hydrogen sulphide has been examined by X-ray single-crystal techniques and shown to have the structure 2,5-dimethyl-2,5-*endo*-thio-1,4-dithiane. The crystals are monoclinic, space group $P2_1/c$, with $a=10{\cdot}970$, $b=6{\cdot}371$, $c=12{\cdot}129$ Å and $\beta=91{\cdot}6°$. The diffraction data were measured using an on-line, automatic, computer-controlled film scanner. Positional and anisotropic thermal parameters of the carbon and sulphur atoms and positional and isotropic thermal parameters of the hydrogen atoms were refined to give a final R value of 0·044.

Introduction

The reaction between an alcoholic solution of chloroacetone saturated with hydrogen chloride and hydrogen sulphide gives the product $C_6H_{10}S_3$. There has been considerable discussion as to the structure of this product, and several different models have been proposed for it (Rappe & Gustafsson, 1967). Böhme, Pfeiffer & Schneider (1942) isolated the substance and proposed the structure 2,6-dimethyl-2,6-*endo*-thio-1,4-dithiane (II). Brintzinger & Ziegler (1948) reported that, from the reaction of chloroacetone, hydrogen sulphide and hydrogen chloride, they had isolated bis-thioacetonyl sulphide; however, Böhme & Schneider (1949) maintained that this product and the one previously reported by them were identical. On the basis of inde-